ACS APPLIED MATERIALS & INTERFACES

Research Article

www.acsami.org

The Fluid Diode: Tunable Unidirectional Flow through Porous Substrates

Joseph E. Mates,[†] Thomas M. Schutzius,[†,‡] Jian Qin,[§] Don E. Waldroup,[∥] and Constantine M. Megaridis*[,†]

[†]Department of Mechanical and Industrial Engineering, University of Illinois at Chicago, Chicago, Illinois 60607, United States

[‡]Department of Mechanical and Process Engineering, Swiss Federal Institute of Technology, Zürich, 8092, Switzerland

[§]Corporate Research and Engineering, Kimberly-Clark Corporation, Neenah, Wisconsin 54956, United States

[∥]Corporate Research and Engineering, Kimberly-Clark Corporation, Roswell, Georgia 30076, United States

Supporting Information

ABSTRACT: Many important applications in fluid management could benefit from unidirectional transport through porous media via a simple, large-area, low-cost coating treatment; in essence, a fluid diode demonstrated herein for water using common cellulosic paper substrates. In electronics, the diode is an electrical component with asymmetric current transfer characteristics. A light (<2 g/m^2) superhydrophobic conformal coating applied onto *one side* of a porous substrate is shown to create a liquid transport function analogous to the electronic diode, facilitating fluid movement in one direction under negligible penetration pressures, but opposing it in reverse up to greater pressures. The phenomenon is driven by capillary action and can be observed using any similarly-thin fluid barrier applied on only one side (i.e., wettability contrast) of an absorbent porous matrix. Diodic action and liquid transport rates are shown to be highly tunable, determined by fiber diameter and spacing, in combination with coating deposition amount. As an example, the device is used to separate an oil/water mixture, relying upon the surface tension differences of the mixture constituents, and may be implemented in multicomponent fluid filtration/separation technologies.

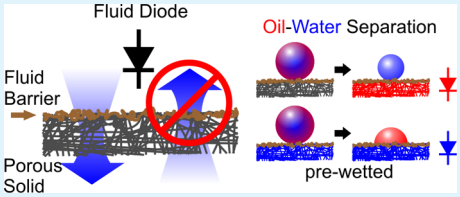

KEYWORDS: *fluid diode, superhydrophobic coating, porous substrate, oil/water separation, flow rectification*

1. INTRODUCTION

The concept of the electronic diode has numerous analogues in fluid management, as the control and rectification of fluid flow is critical for commercial and industrial applications (e.g., check valves) and necessary for life itself (e.g., veins).[1] The diode is an electrical component with asymmetric current transfer characteristics: low resistance in one direction, ideally zero, and high resistance in the other, ideally infinite. Recent literature has extended this concept of diodicity into the realm of microfluidics: the thermal diode,[2] relying on a pair of parallel/opposing superhydrophobic/hydrophilic surfaces under an applied temperature gradient to induce heat transfer in one direction via jumping droplets; valve-less micropumps,[3] utilizing flow rectifiers to generate a net flow in one direction; and superhydrophobic asymmetric ratchet structures,[4] harnessing the Leidenfrost effect for unidirectional droplet transport via vapor flow rectification. A similarly titled paper[5] also exploited open-surface patterned hydrophilic channels on a hydrophobic background for fluidic logic circuits in single-use lab-on-a-chip applications. While these examples highlight analogous diodic behavior, the present device is novel. In addition, due to its inherent simplicity in terms of both fabrication and implementation, the present device is expected to be attractive for wide use in industrial and commercial applications. It is shown that the controlled application of a superhydrophobic treatment onto one side of an absorbent porous substrate imparts tunable fluid diodicity, made possible by competing capillary forces.

The fluid diode is demonstrated herein using a spray-based coating fabrication approach, yet the underlying mechanism requires only a thin, uniform fluid barrier applied onto *one side* of an absorbent (i.e., wicking) porous substrate. The wettability contrast between the coated and uncoated sides of the substrate encountered by the fluid governs fluid flow, or lack thereof, through the material. The degree of repellency and thickness of the fluid barrier, as well as the structure of the porous solid, collectively determine performance (diodicity) of the fluid diode. A water-based superhydrophobic coating formulation[6] is used herein, solely to emphasize the low environmental impact and industry-ready nature of this approach, yet other liquid repellent coatings would behave similarly. Neither the barrier nor the substrate is unique to the operation of diodic fluid transport; greater pressure regimes can be achieved by choosing a substrate of finer pore dimensions than that of the present cellulosic substrates.[7]

Received: May 7, 2014
Accepted: July 2, 2014
Published: July 2, 2014

 © 2014 American Chemical Society

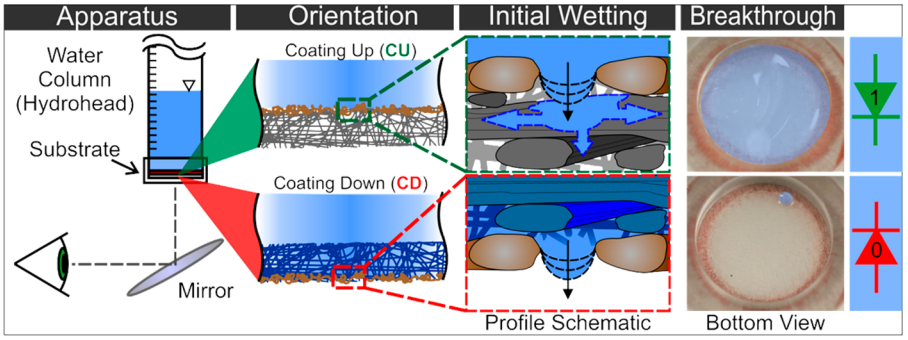

Figure 1. Fluid diode: Depending on the relative orientation of the liquid-repellent coating with respect to the porous wettable solid and the water column (blue) used to impose hydrostatic pressure, the transmission of water through the system will register as a 1 (fluid transmission, coating up, CU in green) or 0 (no fluid transmission, coating down, CD in red), similar to the function of an electronic diode. The CU schematic (top) displays a coated pore under pressure during the initial phase of fluid penetration and a sagging water interface movement (dashed black line in profile schematic). As the imposed hydrostatic pressure increases, the sagging water meniscus extends to the depth of the next uncoated fiber, and once contact is made, fluid wicks through to the underside, imposing no further resistance to the water column above and forming a water film over the entire underside of the substrate *after the penetration pressure has been surpassed* (shown in the breakthrough column, top right). For the CD case, the substrate is completely saturated with water before filling the coated pore; as the sagging water interface extends down under increased external forcing, the threshold pressure is generally much higher than that of CU due to the lack of any additional wettable material in the vicinity beyond the fluid barrier. Eventually, the emerging liquid forms a droplet once the Laplace pressure of the largest pore is exceeded (blue droplet seen in the breakthrough column, bottom right).

The development and application of functional superhydrophobic nanocomposite coatings applied by spray have been well investigated due to their low-cost, large-area capabilities.[8−13] There is great industrial interest to utilize such coatings in the areas of smart fabrics,[14] filtration,[15] pumpless transport,[16] and enhanced heat transfer.[17] In general, these surface treatments are deposited with the goal to impart water resistance and self-cleaning characteristics (apparent contact angle (CA) $\theta^* > 150°$, droplet roll-off angle <10°).[18] It is reported that, at sufficiently low add-on levels, specifically those below 2 g/m^2 (gsm), of a superhydrophobic polymer-nanoparticle composite coating acting as a thin fluid barrier, fluid flow through the underlying porous hydrophilic substrate occurs under low hydrostatic pressures when the liquid encounters the nonwettable coating first, yet fluid flow through the same system is opposed up to greater penetration pressures (i.e., diodic function) if the liquid first encounters the substrate from the opposite (wettable) side. This disparity in the hydrostatic pressures necessary to force the liquid through the porous matrix is the foundation for fluid diode operation.

2. EXPERIMENTAL SECTION

2.1. Substrates. The porous solids used in this study are common paper towels. Paper towels are absorbent cellulosic textiles made from paper and, unlike cloth towels, are disposable and intended to be used only once. Paper towels soak up water because they are loosely woven, enabling water to wick between the fibers, even against gravity. The paper towels used in this study were Kleenex hard roll towels (high-density paper towels; HDPT) and Scott Paper Towel (SPT) (Kimberly-Clark Corp, USA); these two materials were chosen for their low-cost and ubiquitous presence in the marketplace. However, the diode mechanism is substrate-independent and only requires the substrates to be absorbent; they must possess wettable fibers, pores, or channels that allow for fluid wicking by capillary action. If the diode action observed with water is to be repeated for oils, any substrate wettable by oil can be used in conjunction with a thin *superoleophobic* coating applied on one side; the mechanism will remain the same and is to be the subject of future work. For the purposes of this article, displaying functionality on disposable and ubiquitous materials with an environmentally benign coating underscores the inherent simplicity of the mechanism. The present technique can be implemented and further enhanced on more sophisticated substrates possessing specific characteristics, as will be discussed below. Moreover, while oil/water separation has been demonstrated elsewhere using similar superhydrophobic treatments on porous media,[19] it is also shown below that the present coating coupled with a cellulosic substrate can separate not only oil from water but also water from oil if the substrate is properly primed.

2.2. Materials. Bentonite (hydrophilic) nanoclay particles were obtained from Sigma-Aldrich (Product# 682659). The aqueous fluoroacrylic copolymer dispersion (PMC) was obtained from DuPont (20 wt % dispersion in water; Capstone ST-100). Deionized water was used as a probe liquid for characterization and colored with blue food dye to visualize oil/water separation. Hexadecane dyed with Oil Red O, both obtained from Sigma-Aldrich, was used to demonstrate and visualize oil/water separation.

10 mL of sprayable dispersion was prepared as follows. Initially, 0.125 g of nanoclay was added to 9.25 mL of deionized water and bath-sonicated for 15 min (Branson 8200, 20 kHz, 450 W). After sonication, a stir bar was added to the dispersion and 0.625 g of the PMC aqueous solution was added dropwise under mechanical mixing over the course of 1 min to ensure adequate mixing, as the solution became more viscous during this process. The final nanoclay/PMC dispersions (97.5 wt % water, 1.25 wt % PMC, 1.25 wt % nanoclay) were applied by spray onto each substrate using an airbrush atomizer (Paasche, VL siphon feed, 0.55 mm spray nozzle) from a distance of 25 cm. Each spray-pass represented an average of ∼0.5 gsm of conformal coating add-on applied in the typical spray area (9.5 × 7 cm^2). Add-on level was measured by placing glass slides within the spray area, which were then weighed after every pass to determine average coating add-on weight and variance (see the Supporting Information); this base level was used as a gauge for determining approximate coating deposition onto the spatially nonuniform cellulosic substrates under similar conditions. After spraying, the samples were allowed to dry in open air overnight at room temperature.

An added benefit of the present superhydrophobic treatment[7] is that the sprayable dispersion is composed of 97.5% water (see Figures S1 and S2 in the Supporting Information for CA characterization), thereby reducing the adverse environmental impact intrinsic to the synthesis of harsh solvent-based superhydrophobic formulations, and is thus more attractive for industrial implementation. The fluoroacrylic copolymer (PMC) used in this study was created by industry in response to an initiative set forth by the EPA in 2006 to reduce the length of perfluoroalkyl groups in these copolymers, thus eliminating

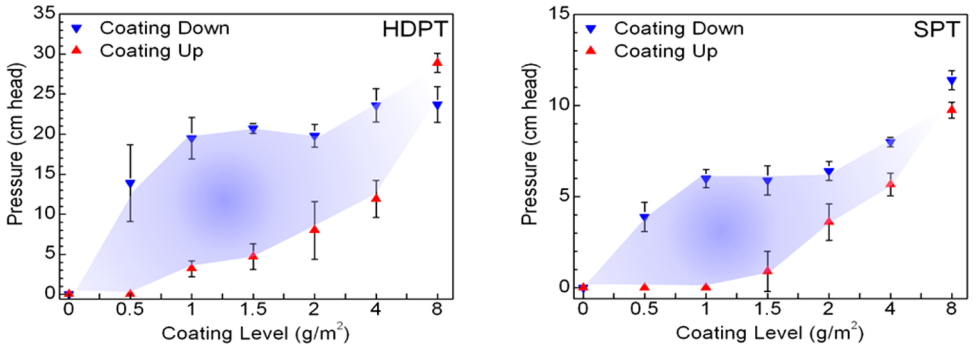

Figure 2. Water pressure penetration resistance versus coating level in gsm for HDPT (left) and SPT (right): The blue downward pointing triangles denote tests conducted coating-side down (CD), while the red upward pointing triangles denote coating-side up (CU) orientation. The disparity in penetration pressures at the lower coating levels suggests fluid flow diodicity, allowing water to pass unimpeded when in the CU orientation, or forward flow, while resisting reverse flow in the CD orientation. The diodicity (i.e., pressure differential) is greater for the HDPT over that of SPT due to the finer fiber structure in the former substrate.

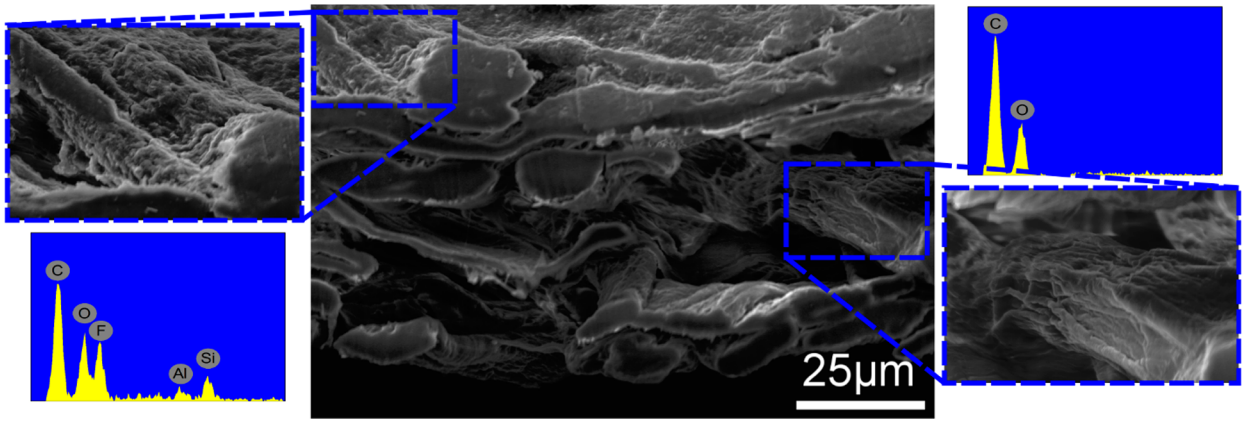

Figure 3. Center: SEM cross-sectional image of HDPT with a 2 gsm superhydrophobic coating on top. The conformal superhydrophobic coating is visible as a thin layer along the top of the cross-section, with the uncoated fibers seen below. The left inset is a close-up of a coated fiber and shows the polymer/clay nanostructure as a roughening of the plain ridged surface of the uncoated fiber (right inset). EDS spectra are included to distinguish the presence of the nanocomposite coating (left) with energy peaks for carbon, oxygen, fluorine, aluminum, and silicon, as compared to the uncoated cellulosic fibers (right) with peaks for carbon and oxygen only. Fluorine is due to the presence of the fluoropolymer matrix, while the nanoclay contains both aluminum and silicon.

precursor chemicals that could break down into perfluoroctanoic acid (PFOA).[20]

2.3. Characterization. The paper towel samples were sprayed on one side only with increasing coating levels ranging from 0.5 to 8 gsm. To demonstrate diodicity, hydrostatic pressure tests (hydrohead; see the Supporting Information, Figure S3) were performed for the same coating weights with the coating up (CU) or coating down (CD), representing forward or reverse flows, respectively (see Figure 1). Thus, diodicity is confirmed if there exists separate and distinct hydrohead thresholds determined by the orientation of the coated side (up or down) for the same coating add-on level. Without any surface treatment, the threshold pressure is naturally zero for both substrates, as water immediately penetrates into and through the paper samples due to their as-received natural absorbency.

3. RESULTS AND DISCUSSION

As can be seen in Figure 2 when testing CU, the coating add-on levels below 1 gsm for HDPT, and below 1.5 gsm for SPT, allow water penetration immediately through the samples under negligible applied pressures; the coating offers near zero penetration resistance. For these lower add-on levels, any water volume greater than a small droplet (10−30 μL) resting on the coated surface is instantaneously absorbed; this is due to insufficiently coated hydrophilic fibers creating an avenue for the wicking of water *through the coated layer*. Under the same add-on levels, Figure 2 shows that the CD orientation delivers nonzero resistance at even the lowest coating of 0.5 gsm for both HDPT and SPT. At this coating level and orientation, the hydrohead threshold is 13.9 ± 4.8 cm head (1.35 kPa) for HDPT and 3.9 ± 0.8 cm head (0.38 kPa) for SPT (the reduced resistance of SPT is due to its larger fiber spacing; see the Supporting Information, Figure S4). The maximum CD/CU pressure disparity was observed at 1 gsm for both substrates, with a difference of ~16 cm head for HDPT and ~6 cm head for SPT, both strongly favoring the CD orientation. These numbers are bounded by the intrinsic Laplace pressure of the effective pore radii,[7] or fiber spacing, in the substrates. At heavier coating levels, the mm-thin substrates become almost entirely hydrophobic due to the absorption of the low surface energy polymer during spraying. Consequently, the threshold pressures for CD/CU converge in Figure 2 as substrate repellency becomes more uniform. Nonetheless, it is important to note that much higher pressure CD/CU differences could be attained by using other porous substrates that feature smaller fiber sizes and much tighter fiber structures, both translating to higher Laplace penetration pressures and thus improved diodicity.

Figure 3 shows an SEM cross-section of HDPT in the center, analogous to the simplified profile schematic in Figure 1. Visible along the upper fiber surfaces, the coating conforms to the fibers and effectively limits access to water except through the fiber spacing or coated pores. The Figure 3 insets clearly show the difference in surface texture between a coated (left) and an uncoated (right) fiber surface along with accompanying EDS (energy dispersive X-ray spectroscopy) spectra verifying the presence of the fluoropolymer coating constituents on the top side. The polymer/clay nanocomposite coating is spread evenly over the top surface fibers; the fluoropolymer film greatly reduces the surface energy (~16.4 mN/m based on probe liquid CA measurements; see the Supporting Information for Owens/Wendt calculations[21]), while the nanoclay features along the intrinsic fiber morphology create a hierarchically textured surface ideal for superhydrophobicity (see the Supporting Information, Figures S4–S5 for additional SEM images of both substrates; Figure S4 offers a comparison of fiber size and spacing for both substrates, while Figure S5 shows images of a single HDPT pore after successive coating applications).

Referring again to Figure 1, the water absorption mechanisms for CU and CD orientations are compared; as hydrohead pressure increases and water is forced into the nonwettable coated layer in both cases, the curvature (i.e., sagging) of the water meniscus increases (see dashed black curves in Figure 1, profile schematic) between the fibers or pore cross-section. Analogous to an electrical circuit, the "flow" current will be in the direction in which the water is introduced over the substrate. The surface that the water encounters first, either the repellent nanocomposite coating (CU) or the absorbent fibers of the substrate (CD), determines the action of the fluid diode: allowing or denying transmission of the current or fluid flow (in binary logic, a 1 or 0). As in electrical diodes, there is a maximum current regime (i.e., imposed hydrostatic pressure in the present case) which, if exceeded, will result in device failure or breakdown; in the case of the fluid diode, operating failure corresponds to leak-through. The threshold pressure is determined as the pressure under which water passes through the coating and substrate, regardless of orientation (CU or CD).

For CU orientation, the pressurized water meniscus first encounters the superhydrophobic coating and begins filling the coated hydrophobic pore(s) as the hydrostatic pressure is increased. The extent of the sagging interface and thus the pressure threshold for fluid penetration into the underlying wettable matrix is bounded by the depth of the next uncoated fiber(s) underneath. Once contact between the sagging water interface and the uncoated fiber(s) beneath the coated pore is made, wicking occurs immediately (blue arrows in Figure 1) and provides an avenue for saturation of the entire substrate and fluid transmission, thus designating the penetration pressure (as shown in the bottom view for CU). However, for the CD orientation, water saturates the hydrophilic fibers it encounters first before it reaches the nonwettable coating (bottom) and begins to emerge through the resistant hydrophobic porous layer separating the wetted fibers from the ambient air. Eventually, as the imposed hydrostatic pressure is increased and the water meniscus sags further into the coated pores (and out of the bottom of the substrate), the threshold pressure is determined by the corresponding Laplace pressure of the spacing between the fibers or pore radii. Once this limit is surpassed, the system can no longer resist the imposed hydrohead above and water emerges in the form of distinct droplets from the pore (see Figure 1, CD bottom view, taken just after threshold pressure was exceeded).

Thus, for CU orientation or forward flow (Figure 1, green diode symbol), the hydrohead threshold is primarily *a function of fiber depth* (λ in Figure 4a) beneath the coated layer and

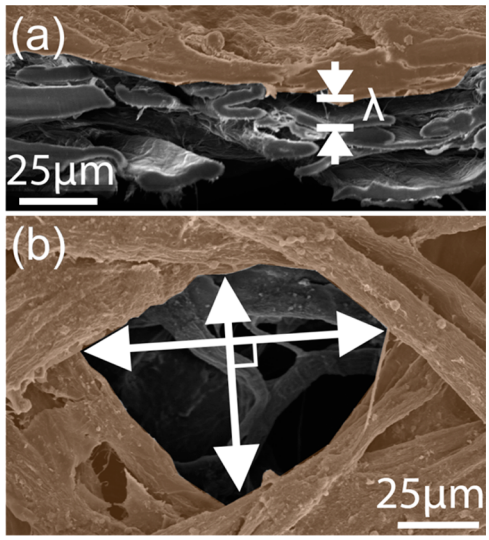

Figure 4. False-color SEM micrographs of HDPT with a 2.5 gsm hydrophobic coating on one side; color has been added to the fluoropolymer coating for better visualization. Fiber spacing results in a disparity between threshold penetration pressures (hydrohead) depending on applied coating orientation, CU or CD. (a) Cross-sectional image (as in Profile Schematic of Figure 1) illustrates the average spacing (λ) between the coated top and the underlying wettable fibers; this spacing represents the maximum distance the liquid meniscus can sag into a coated pore before being wicked throughout the substrate, thus designating the *lower bound of threshold hydrohead in the CU orientation*. (b) Surface image (as in bottom view of Figure 1) illustrates a typical pore that the liquid fills as it emerges from the uncoated side of the substrate and into the surrounding air. The orthogonal minimum and maximum pore dimensions designate the *Laplace pressure and upper bound for the maximum threshold hydrohead in the CD orientation* (in this case, ~38 cm head of water). Both spacing parameters are equally important for determining the upper and lower bounds in the operating range for the fluid diode.

corresponds to a diode logic value of 1 (pass mode), as this orientation (counterintuitively, nonwettable coated-side toward the fluid) facilitates fluid transport at lower pressures. This is verified by calculating the forward threshold pressure (P_{Forward}) required for forcing the sagging meniscus[22] through the coated pore to the depth of the next, uncoated fiber, λ: $P_{\text{Forward}} \approx 2\lambda\gamma/R^2$, where γ is the surface energy of the liquid/vapor interface (~72 mN/m for water) and R is the radius of the pore (i.e., lateral fiber spacing). If a λ-spacing of 10 μm is assumed (see the Supporting Information, Figure S4) for either of the two substrates tested herein, this delivers a negligible forward threshold pressure P_{Forward} below 2.3 cm head (<0.22 kPa). Accounting for variations in the fiber spacing, which may give rise to values of λ well below the assumed 10 μm average depth, a near-zero pressure threshold in the CU orientation can be rationalized and is directly observed (Supporting Information, Figure S4; fluid penetration will occur at the most vulnerable point, i.e., the smallest λ). For thicker coatings, the spacing between fibers allows for excess coating material to penetrate

the pores, thus forming a more torturous path for the water interface to penetrate, as seen in Figure 2 by the converging pressure disparities at higher coating add-ons.

For the inverse CD orientation or reverse flow (Figure 1, red diode symbol), the curved water interface also sags under increased pressure but now advances into open air space beneath the wetted substrate. The CD threshold pressure is no longer dependent on adjacent fiber depth but rather *only on effective pore size* within the coated layer itself (Figure 4b). This orientation corresponds to a diode logic value of 0 (no-pass mode), as fluid transport is impeded below a performance threshold determined by the fiber spacing and corresponding porosity. For the fiber spacing in Figure 4b, the reverse threshold pressure ($P_{Reverse}$) is given by the Laplace pressure $P_{Reverse} = \gamma(1/R_1 + 1/R_2)$, where R_1 and R_2 are the orthogonal minimum and maximum pore radii. This delivers a value of ~38 cm head of water, higher than the observed ~21 cm head but not altogether unexpected. This discrepancy is explained by the existence of a range of fiber spacing in the coated layer, as reverse penetration pressures are determined by the weakest points (i.e., largest pores) in the coated substrate. It is important to emphasize that fluid transport is qualified here in terms of liquid penetrating through the entire coated substrate from the water column side to the opposite (air) side, as shown in the bottom view of Figure 1 for both orientations.

As shown above, the two determining factors, pore size and fiber depth, are equally important and depend on the fiber orientation. The pore size determines the upper bound for the CD orientation and is the more critical factor in determining maximum pressure resistance in reverse flow, whereas the fiber depth λ determines the lower bound in the CU orientation or forward flow. Decreased fiber spacing in either orientation will deliver the best results: low resistance CU and high resistance CD. This suggests a tunable design, where fiber size and packing density (porosity) can be selected for a desired fluid diode operation range. A simple metric for diodicity is the ratio $P_{Reverse}/P_{Forward} \sim R/\lambda$ (R is the average pore radius), which offers guidance for maximizing design performance. For more industrially relevant pressure resistance regimes, the reduction of fiber size/spacing in the absorbent porous medium will increase the corresponding pressure disparity. Thus, for low coating levels, it is possible to achieve a preferred directionality, or "diode window", where a coated porous substrate will permit fluid flow in one direction, but oppose it in reverse for a tunable pressure range.

In general, the applications for controlled diodic fluid transport are abundant, such as any type of filtration where reverse flow contamination is of concern. An example of practical application for fluid diode function would be that of a child's diaper, where the diode barrier can pass relatively large volumes of fluid to an absorbent sub-layer before the hydrostatic threshold pressure is surpassed (i.e., return of fluid in reverse flow or leak-back), with the additional benefit of keeping the surface in contact with the child's skin dry. As fluid contacts the light coating (<2 gsm) in CU orientation, it is absorbed through the insufficient barrier and wicks along the uncoated fibers beneath, yet when the flow is reversed in the CD orientation (e.g., pressure increasing near the saturation point, child sitting, etc.), the same diodic substrate can withstand a much greater pressure without transmitting liquid (leaking) through. It is energetically more favorable for the water to saturate the remaining dry uncoated fibers "laterally" than to overcome the energy barrier created by the conformal coating and leak back through to the opposite (air/skin) side, not to mention more desirable for the parent.

When examining the potential of the fluid diode for multicomponent fluid (i.e., oil/water) separation, it has been shown that many superhydrophobic surfaces remain oleophilic due to the lower surface energy of oils and the lack of re-entrant surface features.[23−25] This difference in surface tensions allows for simple oil/water separation and results in the wicking of oil out of an oil/water mixture and into the underlying substrate, as shown in Figure 5a with top-coated HDPT. In rare

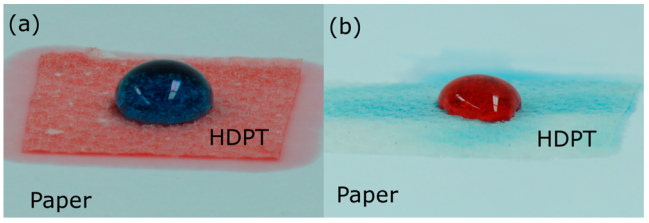

Figure 5. Using the fluid diode (HDPT with 1.5 gsm coating) to selectively separate water (left) or oil (right) from an oil/water mixture: (a) A dry sample is exposed coating-side up (CU) to an hexadecane oil (red)/water(blue) mixture; the oil readily penetrates the light superhydrophobic coating and leaves the water droplet behind on the surface. (b) An identical sample is first saturated with water (undyed for visualization) from the uncoated side. The sample is then exposed CU to the same dyed oil/water mixture, but now resists the oil and allows for water absorption, leaving the oil droplet behind (see Video S1 in the Supporting Information).

examples,[26,27] surfaces can be made both oleophobic and hydrophilic as shown in Figure 5b. A similar substrate to that shown in Figure 5a (fixed coating level of 1.5 gsm; CU orientation) is primed (prewetted) with water from the uncoated side before the oil/water droplet is placed on top. In this case, water (blue) separates from the mixture and leaves the oil (red) behind. Such oil/water separation examples have been shown in the literature for different coatings and/or substrate combinations but not for environmentally friendly and biodegradable materials *in the exact same configuration*. Both images in Figure 5 were obtained for the same coating level (1.5 gsm), orientation (CU), and substrate (HDPT). The liquid separation in Figure 5b was achieved by first saturating the uncoated side with undyed water (undyed water was used to better visualize absorption from the coated side), whereas the substrate in Figure 5a was initially dry. This priming step gives the substrate an oleophobic character, as well as an increased hydrophilicity, due to the saturation of water beneath the thin conformal coating (see Video S1 in the Supporting Information). The hexadecane treated with Oil Red dye had an oil contact angle (OCA) of 0° when tested on the unprimed substrate and ~90° on the primed substrate (Figure 5b). The deionized water was treated with simple blue food dye and had a water contact angle on the superhydrophobic coating greater than 150° (see the Supporting Information).[7] It is interesting to note that, in terms of sliding (roll-off) angles, the 1.5 gsm coating on dry HDPT had a water sliding angle of 15.2 ± 6.2°, yet after absorbing hexadecane oil (oil-wetted) from a mixture, the sliding angle was nearly unchanged at 16.0 ± 6.4°. For oil, in both scenarios for dry and water-wetted substrates, the surfaces were "sticky," as oil droplet mobility was poor.

The demonstrated selective separation of an oil/water mixture suggests further avenues for research where the diode

device can be tailored for fluid-specific separation/filtration applications. As mentioned earlier, to duplicate the diode function for oils, a polymeric substrate, such as polypropylene nonwoven, can be used in conjunction with a light superoleophobic coating treatment, thus allowing for oil flow rectification. In this scenario, separation of multiple low surface energy fluids (preferably <40 mN/m) could be achieved. This, however, is beyond the scope of the present work, which is intended to demonstrate the simplicity of enhanced device functionality with ubiquitous and environmentally benign materials.

4. CONCLUSION

In summary, an effective fluid barrier coating treatment applied on common cellulosic paper substrates has been demonstrated to facilitate fluid diodicity: distinct pressure thresholds depending on the orientation of the substrate coating with respect to the adjacent fluid. The preferred flow directionality resulting from differences in penetration pressure resistance arises due to capillary action, facilitated by the fluid wicking into the absorbent fibers. This technology could be effective in filtration/separation with a wide range of applications, from personal hygiene products to water purification or oil removal. The threshold pressure difference, or "diode window", is highly tunable for application- and fluid-specific designs determined by the choice of substrate, fiber size/spacing, and precision/morphology of the coating. The multicomponent fluid separation method is of practical use to industry for its ability to preselect which liquid is retrieved from a given mixture, as based upon surface energy and priming of the porous solid.

■ ASSOCIATED CONTENT

Supporting Information

Dispersion/application parameters for water-based superhydrophobic formulation; typical images captured during CA measurements on glass slides and HDPT; schematic of hydrohead apparatus; surface free energy of fluoropolymer; SEM images of SPT, top-down and cross-sectional profile, and a typical HDPT pore after successive coatings; video of the fluid diode demonstrating one-way valve operation and oil/water separation in two modes. This material is available free of charge via the Internet at http://pubs.acs.org.

■ AUTHOR INFORMATION

Corresponding Author

*E-mail: cmm@uic.edu. Phone: +1 312 996-3436. Fax: +1 312 413 0447.

Notes

The authors declare no competing financial interest.

■ ACKNOWLEDGMENTS

This material is based upon work supported by Kimberly-Clark Corp. which also contributed the test substrates.

■ ABBREVIATIONS

CA, contact angle
CD, coating side down
CU, coating side up
EDS, energy dispersive X-ray spectroscopy
gsm, grams per square meter (g/m^2)
HDPT, high-density paper towel
OCA, oil contact angle
PFOA, perfluorooctanoic acid
PMC, fluoroacrylic copolymer
SPT, Scott paper towel

■ REFERENCES

(1) Franklin, K. J. Valves in Veins: An Historical Survey. *Proc. R. Soc. Med.* **1927**, *21*, 1−33.
(2) Boreyko, J. B.; Zhao, Y. J.; Chen, C. H. Planar Jumping-Drop Thermal Diodes. *Appl. Phys. Lett.* **2011**, *99*, 234105.
(3) Fadl, A.; Zhang, Z. Q.; Geller, S.; Tolke, J.; Krafczyk, M.; Meyer, D. The Effect of the Microfluidic Diodicity on the Efficiency of Valveless Rectification Micropumps Using Lattice Boltzmann Method. *Microsyst. Technol.* **2009**, *15*, 1379−1387.
(4) Lagubeau, G.; Le Merrer, M.; Clanet, C.; Quere, D. Leidenfrost on a Ratchet. *Nat. Phys.* **2011**, *7*, 395−398.
(5) Chen, H.; Cogswell, J.; Anagnostopoulos, C.; Faghri, M. A Fluidic Diode, Valves, and a Sequential-Loading Circuit Fabricated on Layered Paper. *Lab Chip* **2012**, *12*, 2909−2913.
(6) Megaridis, C. M.; Schutzius, T. M.; Bayer, I. S.; Qin, J. Superhydrophobic Compositions. U.S. Patent 20130030098 A1, January 31, 2013.
(7) Mates, J. E.; Schutzius, T. M.; Bayer, I. S.; Qin, J.; Waldroup, D. E.; Megaridis, C. M. Water-Based Superhydrophobic Coatings for Nonwoven and Cellulosic Substrates. *Ind. Eng. Chem. Res.* **2013**, *53*, 222−227.
(8) Manoudis, P. N.; Karapanagiotis, I.; Tsakalof, A.; Zuburtikudis, I.; Panayiotou, C. Superhydrophobic Composite Films Produced on Various Substrates. *Langmuir* **2008**, *24*, 11225−11232.
(9) Schutzius, T. M.; Bayer, I. S.; Qin, J.; Waldroup, D.; Megaridis, C. M. Water-Based, Nonfluorinated Dispersions for Environmentally Benign, Large-Area, Superhydrophobic Coatings. *ACS Appl. Mater. Interfaces* **2013**, *5*, 13419−13425.
(10) Wu, W. C.; Wang, X. L.; Liu, X. J.; Zhou, F. Spray-Coated Fluorine-Free Superhydrophobic Coatings with Easy Repairability and Applicability. *ACS Appl. Mater. Interfaces* **2009**, *1*, 1656−1661.
(11) Song, H. J.; Shen, X. Q.; Meng, X. F. Superhydrophobic Surfaces Produced by Carbon Nanotube Modified Polystyrene Composite Coating. *J. Dispersion Sci. Technol.* **2010**, *31*, 1465−1468.
(12) Schutzius, T. M.; Bayer, I. S.; Tiwari, M. K.; Megaridis, C. M. Novel Fluoropolymer Blends for the Fabrication of Sprayable Multifunctional Superhydrophobic Nanostructured Composites. *Ind. Eng. Chem. Res.* **2011**, *50*, 11117−11123.
(13) Ogihara, H.; Xie, J.; Okagaki, J.; Saji, T. Simple Method for Preparing Superhydrophobic Paper: Spray-Deposited Hydrophobic Silica Nanoparticle Coatings Exhibit High Water-Repellency and Transparency. *Langmuir* **2012**, *28*, 4605−4608.
(14) Zhou, H.; Wang, H. X.; Niu, H. T.; Lin, T. Superphobicity/philicity Janus Fabrics with Switchable, Spontaneous, Directional Transport Ability to Water and Oil Fluids. *Sci. Rep.* **2013**, *3*, 2964.
(15) Lim, H. S.; Baek, J. H.; Park, K.; Shin, H. S.; Kim, J.; Cho, J. H. Multifunctional Hybrid Fabrics with Thermally Stable Superhydrophobicity. *Adv. Mater.* **2010**, *22*, 2138−2141.
(16) Schutzius, T. M.; Elsharkawy, M.; Tiwari, M. K.; Megaridis, C. M. Surface Tension Confined (STC) Tracks for Capillary-Driven Transport of Low Surface Tension Liquids. *Lab Chip* **2012**, *12*, 5237−5242.
(17) Schutzius, T. M.; Bayer, I. S.; Jursich, G. M.; Das, A.; Megaridis, C. M. Superhydrophobic-Superhydrophilic Binary Micropatterns by Localized Thermal Treatment of Polyhedral Oligomeric Silsesquioxane (POSS)-Silica Films. *Nanoscale* **2012**, *4*, 5378−5385.
(18) Sun, T. L.; Feng, L.; Gao, X. F.; Jiang, L. Bioinspired Surfaces with Special Wettability. *Acc. Chem. Res.* **2005**, *38*, 644−652.
(19) Calcagnile, P.; Fragouli, D.; Bayer, I. S.; Anyfantis, G. C.; Martiradonna, L.; Cozzoli, P. D.; Cingolani, R.; Athanassiou, A. Magnetically Driven Floating Foams for the Removal of Oil Contaminants from Water. *ACS Nano* **2012**, *6*, 5413−5419.

(20) Lau, C.; Butenhoff, J. L.; Rogers, J. M. The Developmental Toxicity of Perfluoroalkyl Acids and Their Derivatives. *Toxicol. Appl. Pharmacol.* **2004**, *198*, 231−241.
(21) Owens, D. K.; Wendt, R. C. Estimation of the Surface Free Energy of Polymers. *J. Appl. Polym. Sci.* **1969**, *13*, 1741−1747.
(22) Tuteja, A.; Choi, W.; Mabry, J. M.; McKinley, G. H.; Cohen, R. E. Robust Omniphobic Surfaces. *Proc. Natl. Acad. Sci. U. S. A.* **2008**, *105*, 18200−18205.
(23) Wang, C. X.; Yao, T. J.; Wu, J.; Ma, C.; Fan, Z. X.; Wang, Z. Y.; Cheng, Y. R.; Lin, Q.; Yang, B. Facile Approach in Fabricating Superhydrophobic and Superoleophilic Surface for Water and Oil Mixture Separation. *ACS Appl. Mater.* **2009**, *1*, 2613−2617.
(24) Lee, C. H.; Johnson, N.; Drelich, J.; Yap, Y. K. The Performance of Superhydrophobic and Superoleophilic Carbon Nanotube Meshes in Water-Oil Filtration. *Carbon* **2011**, *49*, 669−676.
(25) Zhu, Q.; Pan, Q. M.; Liu, F. T. Facile Removal and Collection of Oils from Water Surfaces through Superhydrophobic and Superoleophilic Sponges. *J. Phys. Chem. C* **2011**, *115*, 17464−17470.
(26) Kota, A. K.; Kwon, G.; Choi, W.; Mabry, J. M.; Tuteja, A. Hygro-responsive Membranes for Effective Oil−Water Separation. *Nat. Commun.* **2012**, *3*, 1025.
(27) Zhu, X. Y.; Loo, H. E.; Bai, R. B. A Novel Membrane Showing Both Hydrophilic and Oleophobic Surface Properties and Its Non-fouling Performances for Potential Water Treatment Applications. *J. Membr. Sci.* **2013**, *436*, 47−56.